I.A.U
Karaj branch

Journal of
A p p l ied
C hemical
R esearch
jacr.kiau.ac.ir

Journal of Applied Chemical Research, 18, 1, 8-25 (2024)

An Investigation of the Charge Effects on the Uptake and Release Capacity of Mesoporous Silica Nanoparticles as Vehicles for Short Oligonucleotides

Rafatosadat Badihi[1], Ali Mahmoudi[1*], Mohammad Reza Sazegar[1*], Khodadad Nazari[2]

[1]Faculty of Chemistry, North Tehran Branch, Islamic Azad University, Hakimiyeh, Tehran, Iran

[2]Future Bioenergy Solutions Inc., 369-901 3rd Street West, North Vancouver BC, V7P 3P9, Canada

(Received 20 May 2023; Final revised received 11 Aug. 2023)

Abstract

An easy and cost-effective sol-gel procedure is described for the synthesis and co-modification of mesoporous silica nanoparticles (MSNs) with various metal ions and positive-charge inducing polymers including PEI and PEG, for the construction of a reliable gene delivery vehicle. All of the samples (denoted as PEI-MSN, M-MSN, PEI-M-MSN, and PEG-PEI-MSN, where, M= Fe^{2+}, Fe^{3+}, Co^{2+}, Zn^{2+}, Al^{3+}), were unambiguously characterized by conventional techniques including FTIR, XRD, SEM, and BET. The adsorption capacity of siRNA was found to be more related to the zeta potential of the samples than their specific surface areas. The best adsorption result was obtained by using PEI-Fe(III)-MSN (48.8 µg of siRNA per mg of support). The release of siRNA from PEI-Fe(III)-MSN, was also good (91.5%), but a burst release profile was observed. Interestingly, when a layer of PEG was used as a co-modifier, a sustained release profile was achieved, and meanwhile, the released amount of siRNA was improved (93.2%). The whole combination showed no considerable cytotoxicity according to the MTT test.

Keywords: siRNA, Uptake and release, MSN, Modification, Charge.

[*]***Corresponding authors:*** *Ali Mahmoudi and Mohammad Reza Sazegar, Faculty of Chemistry, North Tehran Branch, Islamic Azad University, Hakimiyeh, Tehran, Iran. Emails: mahmoudiali.ac@gmail.com, m_r_sazegar@yahoo.com.*

Introduction

Gene therapy refers to a method in which modulation of gene expression is premediated in distinct cells for the treatment of diseases. This method serves as a useful approach to selectively affect the pathological issues in certain cells [1]. Since the first human DNA modification attempt by Cline in 1980 [2], the bibliographic records have witnessed the expansion of gene therapy methods using exogenous nucleic acids such as DNA, mRNA, small interfering RNA (siRNA), and microRNA (miRNA). The first therapeutic use of gene delivery was performed by Anderson in 1990. Generally, siRNAs have smaller sizes and less immunogenicity, and these are in favor of overcoming some adverse circumstances. In addition, their development and chemical synthesis is easy to some extent. As an example, potential of siRNA has been approved by injection of Fas siRNA to protect the mice from autoimmune hepatitis [3]. While the siRNA and miRNA oligonucleotides can be used to downregulate the expression of target genes, mRNA can be used for the expression of encoded proteins. Presently, many RNA-based drugs are in clinical trials, and many more are under development. These are intended for the treatment of various diseases including, cancer, liver, neural system, and hereditary diseases [4]. One major concern is the delivery of these oligonucleotides to the target cells, as their physicochemical properties such as negative charge and hydrophilicity preclude their passive diffusion across the plasma membrane. Therefore, this approach faces many physiological barriers such as nucleases, immune cells, non-specific serum proteins, etc. Hence, delivery vehicles are necessary to safeguard NAs, and target them to distinct cells. Inorganic nanoparticles, liposomes, viruses, and polymer-based nano-materials have been recently introduced for efficient gene delivery [5-8]. Silica-based nanoparticles form an outstanding class of inorganic vehicles which have the advantage of good biocompatibility as it is a prerequisite for safe gene delivery [9,10]. Mesoporous silica nanoparticles (MSNs) exhibit a porous honeycomb-like structure of silica. Some interesting advantages of MSNs include tunable size, modifiability, and large specific surface areas (about 1000 m^2g^{-1}). The high surface area of pores paves the way for attachment of certain functional groups on the MSNs [11]. The MSNs fall into three categories, i.e., ordered MSNs, hollow type MSNs, and core/shell type MSNs. Ordered MSNs exhibit their pores arranged in an orderly manner. In order to deliver nucleic acid species, the surface of the MSNs needs to be modified to carry positive charges for the binding of DNA or siRNA. This is achieved by grafting amine groups on the surface [12], coating with polycations such as polyethyleneimine (PEI) [13], and poly(amidoamine) (PAMAM) [14]. Polyethylenimine-polyethylene glycol copolymers (PEI-PEG), also have been used as modifiers for MSNs to co-deliver anticancer agents and siRNA into the breast cancer cells [15]. It has been shown that the nucleic acids are mainly carried by the outer surface of the MSNs [11,16]. In continuation of our

interest and involvement in the chemistry of the MSNs and delivery of short oligonucleotides, herein, we report our study of the surface charge effects on the uptake-and-release capacity of mesoporous silica nanoparticles.

Experimental

Materials

All of the chemicals including $FeCl_2.4H_2O$, $FeCl_3.6H_2O$, $CoCl_2.6H_2O$, $ZnCl_2.3H_2O$, $AlCl_3.6H_2O$, TEOS (98%), CTAB (95%), phosphate buffer (PBS, pH 7.2), NaOH (extra pure), polyethyleneimine (PEI, MW 10 kD), *O, O′*-bis[2-(N-succinimidyl-succinylamino)-ethyl]polyethylene glycol (MW=2000), and absolute ethanol were purchased from Sigma-Aldrich and used as received. siRNA as 21-mer with 3′ TT-overhangs was purchased from Sinagene Co. (Tehran).

Instrumentation

Fourier-transform infrared (FT-IR) spectra were recorded using KBr disks on a Bruker Alpha infrared spectrophotometer. Ultraviolet-Visible (UV-Vis) absorption spectra were recorded on a Varian Cary 100 spectrophotometer in quartz cuvettes. Zeta potentials were measured on a Zetasizer Nano ZS (Malvern, Instruments, Westborough, MA) with a backscattering detection at 173º (25 ºC, 200 µg.mL^{-1}, pH 7.0). Powder X-ray diffraction (PXRD) spectra were recorded on a Philips pw 1830 diffractometer (Cu-Kα X-radiation, λ = 1.54 Å). A JEOL JEM-2100 transmission electron microscope was used for TEM imaging. N_2 adsorption-desorption isotherms were measured at 77 K on a BELSORP MINI II instrument. Samples were degassed *in-vacuo* and annealed at 120 ˚C for at least 6 h to remove moisture. The pore size distribution was determined by the Barrett–Joyner–Halenda (BJH) model.

Methods

Synthesis of mesoporous silica nanoparticles (MSNs)

The general procedure for the preparation of the mesoporous silica nanoparticles is reported earlier [17]. Accordingly, a solution of CTAB (7.29 g) in 175 mL of double distilled water was prepared at room temperature. Then 25% ammonia (13.9 mL) in 228 mL of ethanol, was added to the aforementioned solution and stirred for 1 h. After the addition of 15 mL of TEOS to the mixture and stirring for 5 h, the gel was aged for 2 days. The precipitate was then washed with water and ethanol (100 mL of each), oven-dried at 100 ºC, and finally calcined at 550 °C.

2.3.2. Metal-modification of MSNs

0.1 g of MSN was added to a solution of each of the $FeCl_2.4H_2O$, $FeCl_3.6H_2O$, $CoCl_2.6H_2O$, $ZnCl_2.3H_2O$, and $AlCl_3.6H_2O$ salts to obtain the desired Si/M molar ratio of 75. The suspension was sonicated for 15 min and then stirred at 300 rpm for 5 h at 70 ^oC. The precipitate was then filtered and washed three times with water, oven-dried at 90 °C for 24 h, and finally calcined at 550 ^oC for 3h. The obtained samples were denoted as M-MSN (M= Co^{2+}, Fe^{2+}, Fe^{3+}, Zn^{2+}, and Al^{3+} [18].

Modification of the M-MSN samples with polyethyleneimine (PEI)

The M-MSN samples were covered with a layer of PEI according to the literature [19]. A dispersion of 5.0 mg of the M-MSN in 1.0 mL of absolute ethanol was prepared by sonication for 15 min. Then, 2.5 mg of polyethyleneimine (PEI, MW = 10 KD) was added and the mixture was stirred at 250 rpm for 5 h at room temperature. The PEI-modified particles were collected by centrifugation, washed with absolute ethanol and distilled water (3×10 mL of each), and finally dried at room temperature. The samples were denoted as PEI-M-MSN.

2.3.4. PEG-modification of the PEI-M-MSN

O, O′-bis[2-(N-succinimidyl-succinylamino)-ethyl]polyethylene glycol (NHS terminated PEG, MW= 2000) was added to a dispersion of PEI-M-MSN nanoparticles in ethanol [37]. After stirring for 3 h at room temperature, the conjunction product was filtered-off and denoted as PEG-PEI-M-MSN.

siRNA adsorption-desorption experiments

A specified amount of each support (MSN, M-MSN, PEI-M-MSN, and PEG-PEI-M-MSN) was treated with siRNA solution, and the adsorbed amount was determined by measuring the siRNA concentration in the supernatant solution at different time intervals over 48 h. A standard calibration curve of the absorbance *vs.* concentration was first plotted by measuring the absorbance of siRNA solutions with known concentrations of 1, 5, 25, 50, 75, 100, and 150 μg mL^{-1}, in PBS at 260 nm. The siRNA concentration was then calculated as: [siRNA] = 0.0192 × Abs(260) – 0.037, (R^2 = 0.9976), where Abs(260) is the absorbance of the solution at 260 nm (Figure 1).

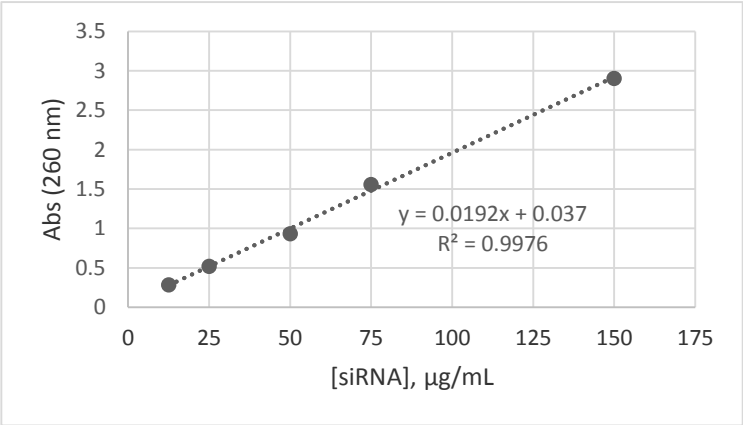

Figure 1. The calibration curve for determination of siRNA.

Cell culture

Normal human fibroblast cells were purchased from the Pasteur Institute of Iran. 200 µL of each of 250 and 125 µg. mL^{-1} concentrations of the MSN-based vehicle in a complete culture medium were introduced into a 96-well plate. Three replicates were performed for each concentration. Then, the trypsinized fibroblasts were suspended, and to each house, 7×10^3 cells were added. Then they were incubated under standard conditions for 24 and 48 h. Afterward, 50 µL of MTT solution (5 mg/mL) was used and wells were re-incubated for 4 h. After the complete dissolution of Formazan crystals by isopropanol, the absorbance was measured at 570 nm. The results were expressed as survival percent ± standard deviation.

Results and discussion

Characterizations

FT-IR study

FT-IR spectra of the MSN and its metal-, and polymer-modified descendants are shown in Figure 2. All of them are in common with the O–H stretching and bending vibrations of water molecules or surface silanol groups at about 3450 and 1640 cm^{-1} [20]. Symmetric and asymmetric vibrations of the Si–O–Si scaffolds were appeared at 1082 and 802 cm^{-1}, respectively. Polymer-modified samples showed the C-H stretching vibrations at about 2970 and 2890 cm^{-1}. Metal-oxide vibrations in tetrahedral holes appeared at about 465 cm^{-1}. Clearly, these bands tend to shift to higher wave numbers upon increasing the oxidation state of the metal. This can be easily seen from the spectra of Fe(II)-MSN and Fe(III)-MSN, and their polymer-modified forms. The C-N stretching vibrations

of the PEI moiety probably overlapped with the strong peaks of the Si-O-Si vibrations (1000-1250 cm^{-1}). It can be concluded that the mesoporous structure of the MSNs was preserved after modification.

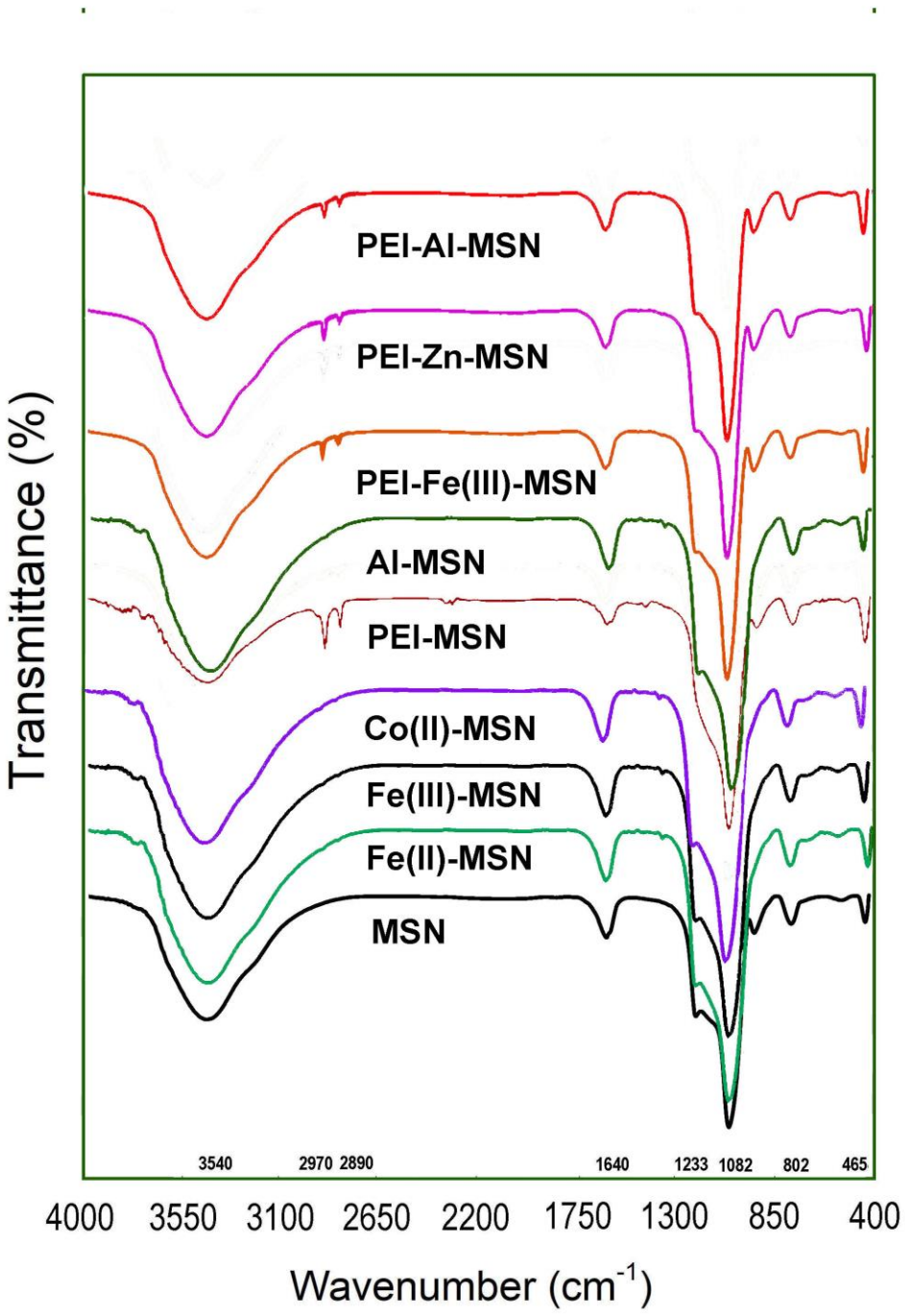

Figure 2 FTR spectra of the MSN and its metal-, and polymer-modified forms.

XRD patterns

Low and high-angle XRD patterns of the MSN and its metal-, and polymer-modified forms are presented in Figure 3. All of the samples exhibit a broad peak at about 22°, resulting from amorphous silica (Fig. 3b) [11]. Clearly, the XRD patterns of metal-, and polymer-modified samples were the same at high angles. In the low angle patterns, a strong diffraction peak at 2.65° corresponding to the (100) plane of the MSN unit cell (Figure 3a), along with two weak reflections at 4.3° and 4.8° attributable to the (110) and (200) planes of the hexagonal mesoporous structure is indicative of a well-ordered mesoporous silica material. Metal modification, however, resulted in the down-shift of the most intense peak to smaller 2θ angles, as a result of the substitution of Si by M^{n+} and increased d_{100} spacing. Polymer-modified MSNs and M-MSNs, however, showed the same XRD patterns, since polymer modification does not affect the crystal structure of the prepared scaffolds. This can be easily understood from the XRD pattern of the PEI-M-MSN samples. It is also noteworthy that the oxidation state of the metals had no drastic effect on the XRD patterns, for example, PEI-Fe(II)-MSN and PEI-Fe(III)-MSN, as presented in Figure 3a.

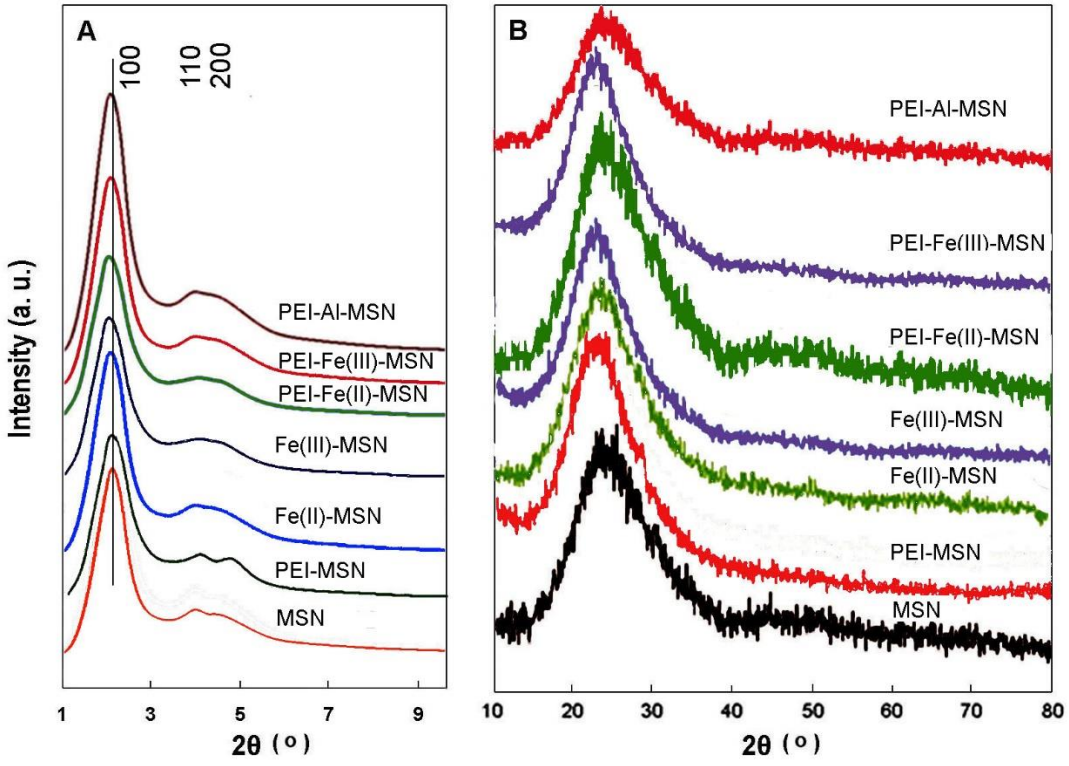

Figure 3 Low (a), and high angle (b) XRD patterns of the MSN and its modified forms.

SEM micrographic study

SEM micrographs of the MSN and its modified forms at 100 kx magnification are shown in Fig. 4. The MSN nanoparticles appeared as uniform spheres in the range of 50-100 nm (Figure 4a). SEM micrographs of the PEI-MSN, Fe(II)-MSN, Fe(III)-MSN, PEI-Fe(II)-MSN, and PEI-Fe(III)-MSN are also presented (Figures 4b-f). One can note that the morphological aspects of the modified forms are not considerably changed, and the spherical shape of the modified MSNs was almost preserved. A negligible increase in the average particle size can be attributed to the increase of *d-100* spacing, as deduced from the XRD patterns. The SEM images of the other products including Co(II)-MSN, PEI-Co(II)-MSN, Al-MSN, and PEI-Al-MSN were more or less the same, and are not presented here for the sake of brevity.

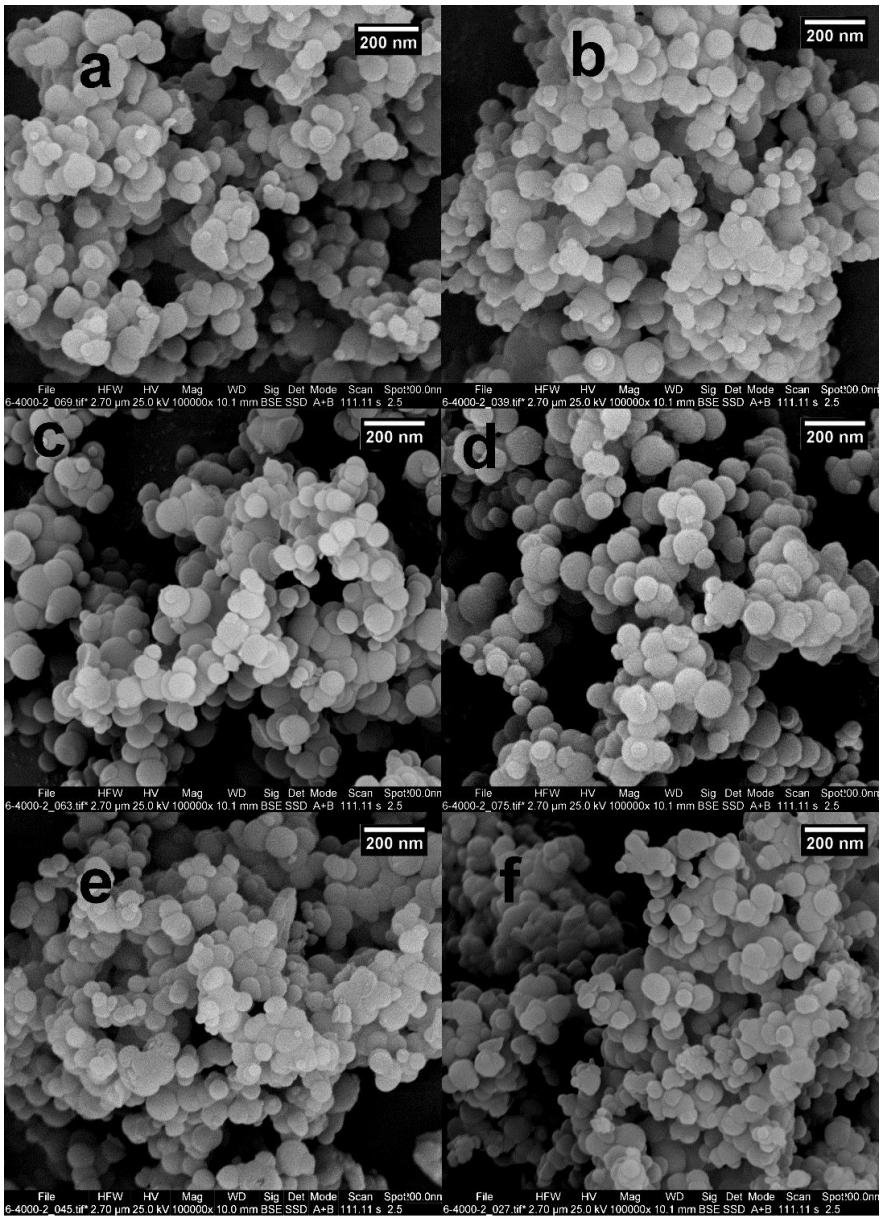

Figure 4. SEM micrographs of the MSN, PEI-MSN, Fe(II)-MSN, Fe(III)-MSN, PEI-Fe(II)-MSN, and PEI-Fe(III)-MSN (a-f).

Nitrogen adsorption-desorption measurements

The effect of the modifiers on the porosity and surface areas of the samples was studied by nitrogen adsorption-desorption measurements. The corresponding N_2-sorption isotherms are shown in Figure 5. All of the samples showed a type IV isotherm with distinct H4 hysteresis loops in the p/p_0 range of 0.3-1.0, corresponding to well-ordered mesoporous materials. The presence of small pores is evident from the sharp inflections of capillary condensation at lower relative pressure. As plotted in Fig. 5, and in agreement with the FTIR, SEM, and XRD results, the mesoporous silica nanoparticles subjected to metal or polymer modification, maintain their crystal and pore structure. Considerable changes in the physicochemical properties of the modified samples, however, were observed as presented in Table 1.

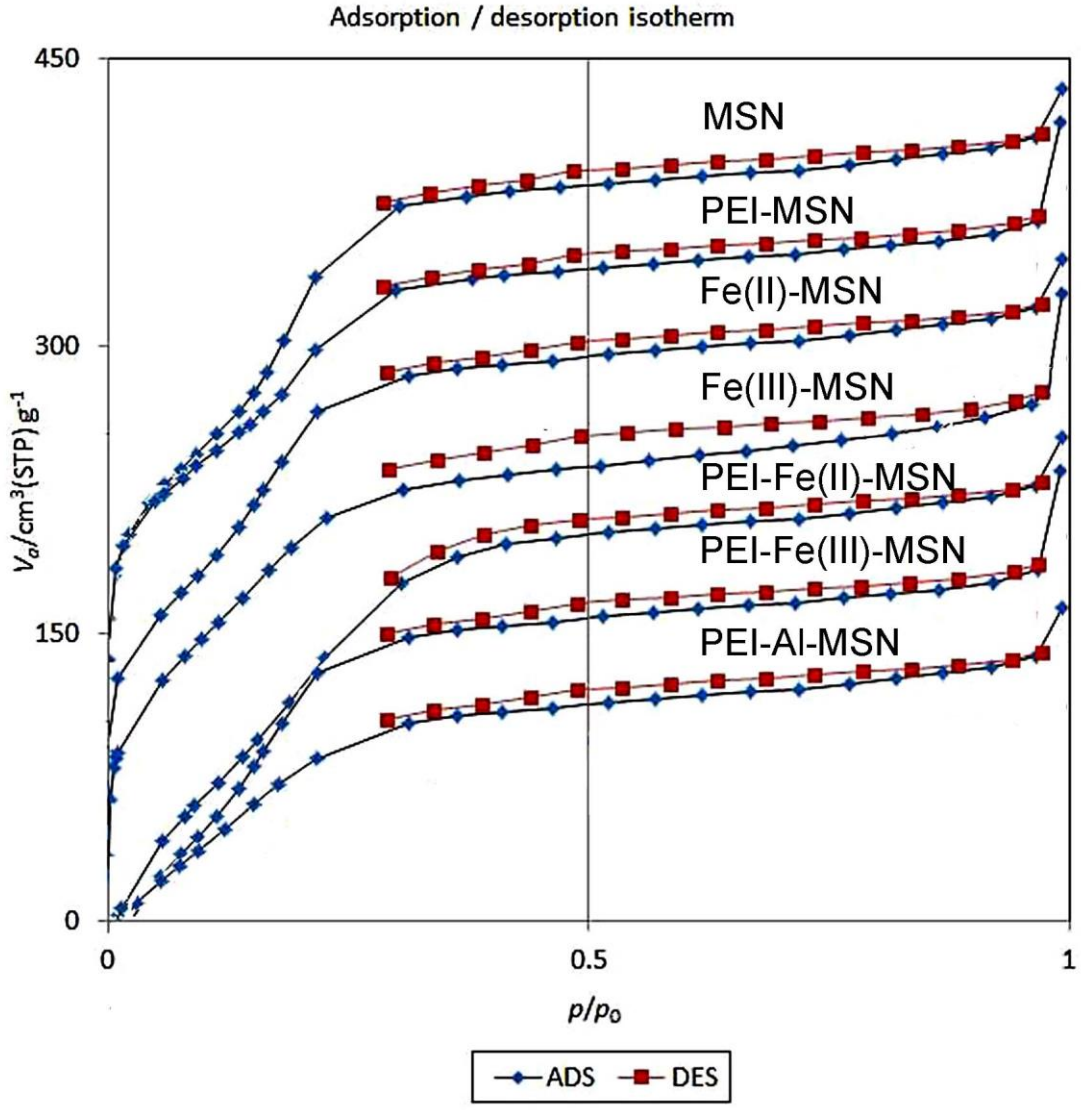

Figure **5** Nitrogen adsorption-desorption isotherms of MSN and its modified forms.

Table 1. Physicochemical properties of the synthesized samples.

Catalyst	S_{BET} [a] (m^2g^{-1})	V_p [b] (cm^3g^{-1})	W [c] (nm)	Average pore diameter (nm)	V_m [d] (cm^3g^{-1})
MSN	1062.2	0.5285	1.21	1.09903	244.05
Fe(II)-MSN	820.12	0.3365	1.21	1.09803	228.10
Fe(III)-MSN	835.05	0.3617	1.16	1.09901	231.02
Co(II)-MSN	784.95	0.3394	1.34	1.09704	230.11
Al-MSN	814.00	0.3212	1.42	1.09900	234.14
Zn-MSN	798.54	0.3210	1.19	1.09888	229.31
PEI-MSN	620.14	0.2987	1.14	1.07806	214.89
PEI-Fe(III)-MSN	486.66	0.2898	1.09	1.07754	212.36
PEI-Al-MSN	512.11	0.2999	1.19	1.07642	218.20
PEI-Zn-MSN	499.87	0.2891	1.03	1.07801	211.24

[a] BET surface area obtained from N_2 adsorption-desorption isotherms; [b] Total pore volume; [c] Pore size obtained from the BJH method; [d] Adsorbed volume.

According to the data in Table 1, the specific surface area (S_{BET}) of the MSN decreased drastically upon polymer modification (1062 *vs.* 620 m^2g^{-1}). This can be attributed to the partial blockage of the pores, as indicated by the total pore volume (V_p, cm^3g^{-1}). The pore blockage is much less when the MSN is modified only with metals. In contrast, modification with both metal and polymer modifiers results in a considerable decrease in the total pore volume and specific surface areas. The effect of the oxidation state of the metal on the physicochemical properties of the sample was not easy to justify. For example, the specific surface area of the Fe(III)-MSN was higher than the Fe(II)-MSN. The same trend was observed for the monolayer adsorbed volume (V_m) and the pore size obtained from the BJH method.

Zeta potential measurements

The measured Zeta potentials for the synthesized samples are presented in Figure 6. All of the modified samples had positive zeta potentials, which is in agreement with previous reports [21]. Changing the values from negative to positive indicates an increase in the MSNs' surface isolation [22]. The zeta potential of MSN was changed from −16.4 mV to +6.0 mV after amination with PEI, making it possible to load siRNA molecules through electrostatic attractions. Metal ions also, can modify the electrostatic nature of the MSNs, and increase the adsorption of siRNA onto their

surfaces by the mediation of the electrostatic repulsions [23]. The observed zeta potential trend is as follows: MSN<PEI-MSN<Fe(II)-MSN<Co(II)-MSN<Zn-MSN<Al-MSN<Fe(III)-MSN<PEI-Al-MSN<PEI-Fe(III)-MSN. One can note that increasing the oxidation state of the metal modifier in combination with PEI results in the highest possible zeta potential values, and the best result was obtained by the Fe^{3+} cations, probably as a result of its smaller ionic radius [24].

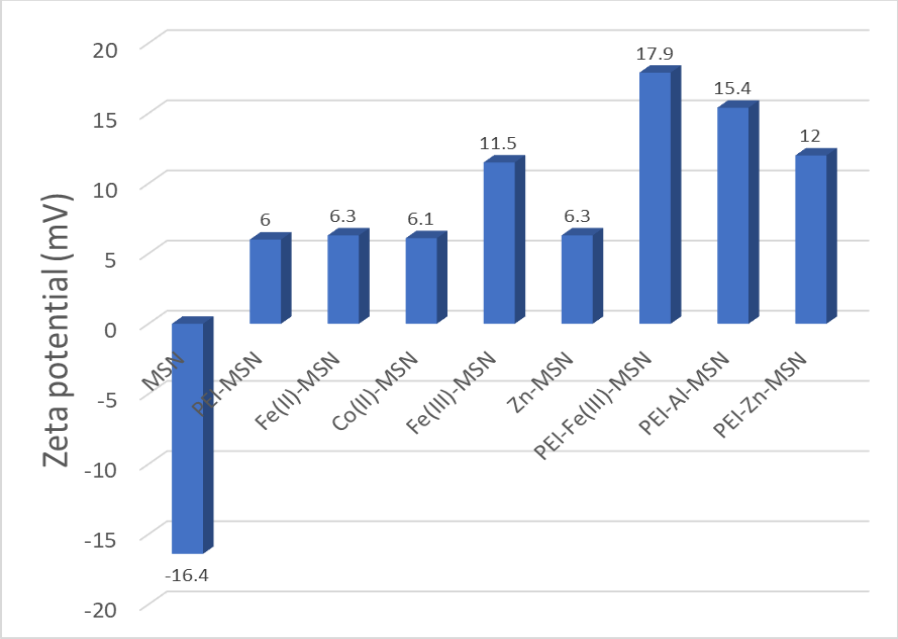

Figure 6. Zeta potential values of the MSN and its modified forms.

siRNA loading studies

UV-Vis spectroscopy was used to study the trend of siRNA adsorption on the MSN and its modified forms. Experimentally, 10.0 mg of each sample was dispersed in 10.0 mL of a 150 µg/mL solution of siRNA in PBS (pH 7.2) at room temperature for 2 h. At given time intervals, the mixture was sampled, filtered, and the absorbance of the filtrate was measured at 260 nm. The corresponding details are described in section 2.3.4. First of all, the maximum loading capacity was determined for each MSN sample after 120 min. This was necessary to limit our study to the best adsorbent, prior to determination of its adsorption profile. The amount of siRNA loaded on the MSN and its modified forms are presented in Figure 7. It is crystal clear that the highest siRNA loading is related to the PEI-Fe(III)-MSN. Considering the physicochemical properties, including specific surface area, along with the zeta potential of the samples, it is clear that the main role is played by the electrostatic charge of the nanoparticles. For example, although the bare MSN has the

highest S_{BET}, its loading capacity is much lower than the others as a result of its surface negative charge and zeta potential. The other data presented in Table 1 also indicate that although the MSN has the highest mono-layer adsorbed volume among the samples, it has the lowest siRNA adsorption capacity. Regardless of the MSN, the adsorption capacity of PEI-M-MSN samples can be somehow related to their S_{BET}, V_m, and average pore diameter values. It can be concluded that although the surface area is an important factor in adsorption experiments, in the case of the modified MSNs, the zeta potential of the nanoparticles has the highest impact on their adsorption capacity. Under the optimized conditions, the highest load of siRNA was 48.8 µg per mg of the PEI-Fe(III)-MSN after 120 min.

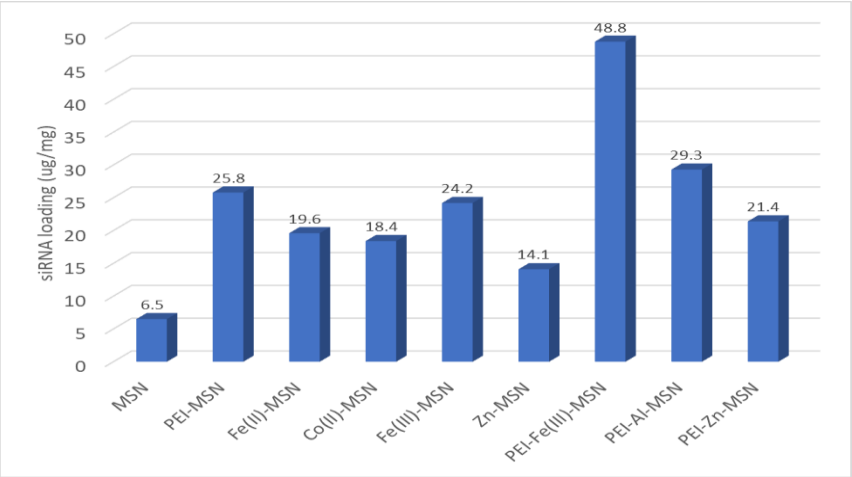

Figure 7. Maximum loading of the siRNA on MSN samples after 120 min. under the optimized conditions.

To study the adsorption profile of siRNA onto the PEI-Fe(III)-MSN, the adsorbed amount was plotted against time over a period of 120 min. Figure 8 shows that the adsorption of the siRNA is fast at the early moments of the treatment and finally reaches a maximum of 48.8 µg/mg after 120 min. This can be announced as a significant promotion when the recent reports in this context are considered [13,25].

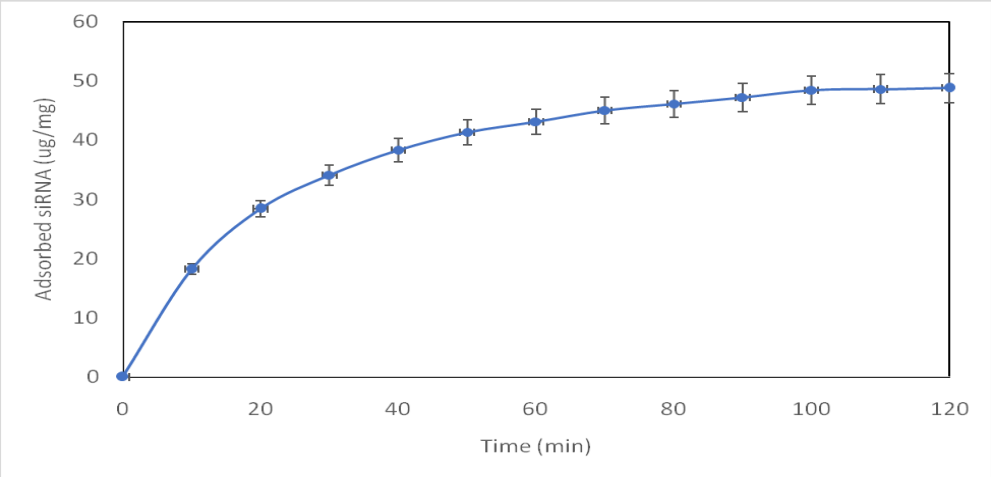

Figure 8. Adsorption profile of siRNA onto the PEI-Fe(III)-MSN within 120 min.

The release of siRNA

To study the release profile, siRNA-saturated PEI-Fe(III)-MSN was first prepared as described in 3.3. After treatment with 20 mL of ethanol and 20 mL of distilled water, the sample was dried *in vacuo*. The resulting siRNA -saturated sample was then dispersed in 1.0 mL of PBS and stirred at room temperature for 2 h. At given time intervals, the mixture was sampled, centrifuged at 5000 rpm for 5 min, and the absorbance of the supernatant was measured at 260 nm. The amount of the released siRNA from the sample was determined as described in section 2.3.4.

Figure 9 shows the release profile of siRNA over 120 min from PEI-Fe(III)-MSN. Clearly, a burst release was happened within the early moments of the experiment, and then reached to a maximum of 91.5% of the adsorbed amount after 120 min. It is well known that a burst release of the therapeutic agents from the vehicle in drug delivery systems is not favorable [26]. Instead, a sustained release profile is usually of great importance [27]. The ease of siRNA release from a modified MSN surface is just as important as its adsorption in siRNA purification techniques and largely depends on the solvent used. The addition of PBS buffer solution reduces the interaction between metal ions and siRNA, and the release of siRNA molecules is facilitated as a consequence. As said before, a sustained release of the loaded components on any vehicle is of crucial importance in drug delivery systems. To overcome this problem, the siRNA-loaded vehicle was treated with a layer of PEG polymer conjugated to the free amines on the particles' surface. It has been shown that the specific surface area, total pore volume, and pore size values decrease drastically upon PEGylation [19]. However, it should be mentioned that the PEG-silane functionalized materials show the blockage effects to a lesser extent [28]. As a consequence of pore blockage by PEG, an additional PEG cleavage step at the expense of time is necessary to release the siRNA in a sustained manner. Therefore, PEGylation of the modified MSNs can be considered a preferred choice for controlling the release profile of the adsorbed nucleotides on the modified MSNs.

To improve the release profile of the siRNA from PEI-Fe(III)-MSN, the effect of pegylation was studied. Interestingly, it was found that co-modification of the Fe(III)-MSN with both PEI and PEG, results in a more adsorption capacity (52.7 µg/mg of support), and meanwhile, the release profile improved considerably as shown in Figure 10. Another advantage of the co-modification of Fe(III)-MSN with both PEI and PEG, is the improvement of the released amount of siRNA. Under the optimized conditions, 93.2% of the adsorbed siRNA was released from PEG-PEI-Fe(III)-MSN after 120 min.

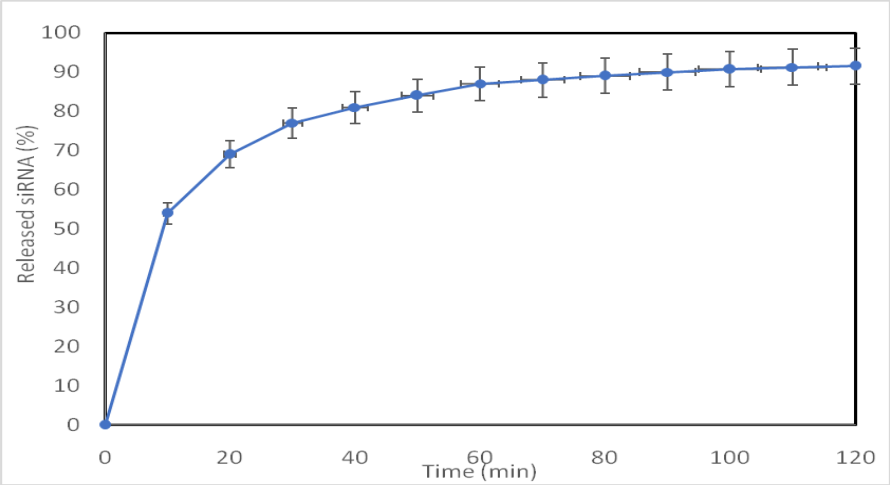

Figure 9. Release profile of siRNA from PEI-Fe(III)-MSN within 120 min.

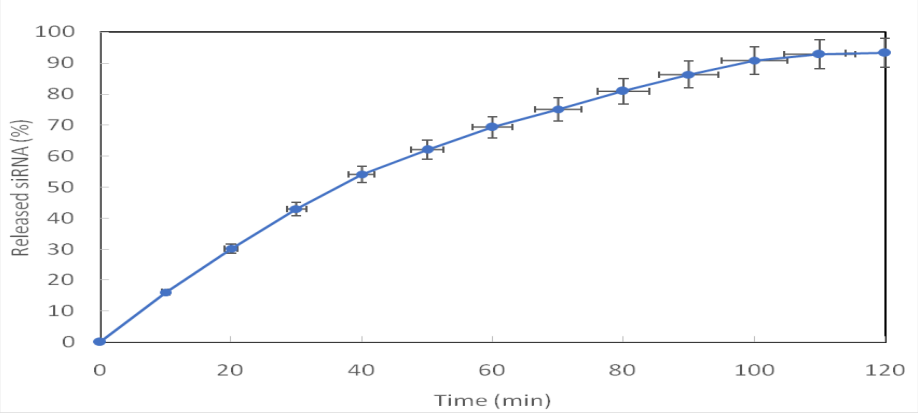

Figure 10. Release profile of siRNA from PEG-PEI-Fe(III)-MSN over 120 min.

Since cytotoxicity is an important issue in gene delivery studies, we decided to study the cell toxicity of the PEG-PEI-Fe(III)-MSN against normal human fibroblast cells as a representative cell line. MTT test was used according to Mosmann's method [29]. Cells were stored in RPMI medium with 10 % FBS and 1 % penicillin/streptomycin under standard conditions (37 ^{o}C and 5 % CO_2) in an incubator. The culture medium was changed every 2 days. After 24 and 48 h of incubation of

cells in presence of different concentrations of the PEG-PEI-Fe(III)-MSN, the MTT results were fetched as summarized in Table 2.

Table 2. MTT results after 24 and 48 h of incubation of normal fibroblast cells in presence of different concentrations of PEG-PEI-Fe(III)-MSN.

Concentration (μg. mL^{-1})	Survival after 24 h (%) [1]	Survival after 48 h (%) [1]
250	96.6	91.1
125	98.9	94.5
62	99.5	96.8

[1] In each concentration, three measurements were carried out.

It is clear that the PEG-PEI-Fe(III)-MSN nanoparticles are tolerable according to the cell toxicity measures announced by Fry *et al* [30].

Conclusion

It can be concluded that sol-gel synthesis of mesoporous silica nanoparticles, followed by co-modification with metals and positive-charge inducing polymers, provides a cost-effective and easy protocol for the preparation of a reliable gene delivery vehicle. The adsorption capacity was found to be more related to the zeta potentials than the specific surface areas. Considering the metal moiety, it was found that the siRNA adsorption capacity depends on the oxidation state of the metal ion. The measured zeta potentials were also relevant to the oxidation state of a certain metal ion. The cationic nature of the PEI modifier, on the other hand, resulted in a higher zeta potential for the modified samples. On the contrary, it was revealed that the physicochemical properties of the MSN support, including specific surface area, total pore volume, and average pore diameter, do not significantly improve the maximum loading. The whole combination showed no considerable cytotoxicity according to the MTT test. The novel features of the present study can be announced as follows: comparison of the different oxidation states of the metal modifier, co-modification with metal ions and positive charge-inducing polymers, discrimination between the role of the surface charge and the surface area, in the uptake and release capacity of the MSNs. Like any other scientific research, the present work may also have some drawbacks. The most important issue is that the PEI is regarded as a quite toxic polymer. Although our study showed no cytotoxicity for the PEI-included vehicles, the final fate of this substance and other ingredients and their excretion from

the body should be studied. In addition, application of other transition metal ions is suggested for further research.

Acknowledgments

We thank the deputy of the research, Tehran North Branch, Islamic Azad University for support of this study.

Declarations

The authors of this manuscript declare no conflict of interest.

References

1. Yin H, Kanasty RL, Eltoukhy AA, Vegas AJ, Dorkin JR, Anderson DG. Non-viral vectors for gene-based therapy. Nature Reviews Genetics. 2014;15(8):541-55.

2. Rosenberg SA, Aebersold P, Cornetta K, Kasid A, Morgan RA, Moen R, Karson EM, Lotze MT, Yang JC, Topalian SL, Merino MJ. Gene transfer into humans—immunotherapy of patients with advanced melanoma, using tumor-infiltrating lymphocytes modified by retroviral gene transduction. New England Journal of Medicine. 1990;323(9):570-8.

3. Wittrup A, Lieberman J. Knocking down disease: a progress report on siRNA therapeutics. Nature Reviews Genetics. 2015;16(9):543-52.

4. Wang KE, Chen W, Zhang Z, Deng Y, Lian JQ, Du P, Wei D, Zhang Y, Sun XX, Gong L, Yang X. CD147-spike protein is a novel route for SARS-CoV-2 infection to host cells. Signal transduction and targeted therapy. 2020;5(1):283.

5. Zeng H, Little HC, Tiambeng TN, Williams GA, Guan Z. Multifunctional dendronized peptide polymer platform for safe and effective siRNA delivery. Journal of the American Chemical Society. 2013;135(13):4962-5.

6. Zhang Y, Ren K, Zhang X, Chao Z, Yang Y, Ye D, Dai Z, Liu Y, Ju H. Photo-tearable tape close-wrapped upconversion nanocapsules for near-infrared modulated efficient siRNA delivery and therapy. Biomaterials. 2018;163:55-66.

7. Van Bruggen C, Hexum JK, Tan Z, Dalal RJ, Reineke TM. Nonviral gene delivery with cationic glycopolymers. Accounts of Chemical Research. 2019;52(5):1347-58.

8. Li Z, Zhang Y, Feng N. Mesoporous silica nanoparticles: synthesis, classification, drug loading, pharmacokinetics, biocompatibility, and application in drug delivery. Expert opinion on drug delivery. 2019;16(3):219-37.

9. Zhou Y, Quan G, Wu Q, Zhang X, Niu B, Wu B, Huang Y, Pan X, Wu C. Mesoporous silica nanoparticles for drug and gene delivery. Acta pharmaceutica sinica B. 2018;8(2):165-77.

10. Shao D, Lu MM, Zhao YW, Zhang F, Tan YF, Zheng X, Pan Y, Xiao XA, Wang Z, Dong WF, Li J. The shape effect of magnetic mesoporous silica nanoparticles on endocytosis, biocompatibility and biodistribution. Acta biomaterialia. 2017;49:531-40.

11. Hajiagha NG, Mahmoudi A, Sazegar MR, Pouramini MM. Synthesis of cobalt-modified MSN as a model enzyme: Evaluation of the peroxidatic performance. Microporous and Mesoporous Materials. 2019;274:43-53.

12. Kneuer C, Sameti M, Haltner EG, Schiestel T, Schirra H, Schmidt H, Lehr CM. Silica nanoparticles modified with aminosilanes as carriers for plasmid DNA. International journal of pharmaceutics. 2000;196(2):257-61.

13. Badihi R, Mahmoudi A, Sazegar MR, Nazari K. A study on co-modification of MSNs with some transition metals and polyethyleneimine (PEI) as a versatile strategy for efficient delivery of short oligonucleotides. Chemical Papers. 2022;76(11):7023-35.

14. Slowing II, Vivero-Escoto JL, Wu CW, Lin VS. Mesoporous silica nanoparticles as controlled release drug delivery and gene transfection carriers. Advanced drug delivery reviews. 2008;60(11):1278-88.

15. Teo PY, Cheng W, Hedrick JL, Yang YY. Co-delivery of drugs and plasmid DNA for cancer therapy. Advanced drug delivery reviews. 2016;98:41-63.

16. Xu W, He W, Du Z, Zhu L, Huang K, Lu Y, Luo Y. Functional nucleic acid nanomaterials: development, properties, and applications. Angewandte Chemie International Edition. 2021;60(13):6890-918.

17. Nakamura T, Mizutani M, Nozaki H, Suzuki N, Yano K. Formation mechanism for monodispersed mesoporous silica spheres and its application to the synthesis of core/shell particles. The Journal of Physical Chemistry C. 2007;111(3):1093-100.

18. Ma Z, Guan Y, Liu H. Superparamagnetic silica nanoparticles with immobilized metal affinity ligands for protein adsorption. Journal of Magnetism and Magnetic Materials. 2006;301(2):469-77.

19. von Baeckmann C, Kählig H, Lindén M, Kleitz F. On the importance of the linking chemistry for the PEGylation of mesoporous silica nanoparticles. Journal of Colloid and Interface Science. 2021;589:453-61.

20. Mardani F, Khorshidi A, Gholampoor S. Sulfonated Caspian Sea Sand: A Promising Heterogeneous Solid Acid Catalyst in Comparison with–SO3H Functionalized NiFe2O4@ SiO2@ KIT-6. ChemistrySelect. 2019;4(27):8015-20.

21. Akbarzadeh M, Oskuee RK, Gholami L, Mahmoudi A, Malaekeh-Nikouei B. BR2 cell penetrating peptide improved the transfection efficiency of modified polyethyleneimine. Journal of Drug Delivery Science and Technology. 2019;53:101154.

22. Lindén JB, Larsson M, Kaur S, Nosrati A, Nydén M. Glutaraldehyde-crosslinking for improved copper absorption selectivity and chemical stability of polyethyleneimine coatings. Journal of Applied Polymer Science. 2016;133(37).

23. Ganguly A, Ganguli AK. Anisotropic silica mesostructures for DNA encapsulation. Bulletin of Materials Science. 2013;36:329-32.

24. Zhang X, Zhang J, Quan G, Yang P, Pan X, Wu C. The serum-resistant transfection evaluation and long-term stability of gene delivery dry powder based on mesoporous silica nanoparticles and polyethyleneimine by freezing-drying. AAPS PharmSciTech. 2017;18:1536-43.

25. Kim H, Yuk SA, Dieterly AM, Kwon S, Park J, Meng F, Gadalla HH, Cadena MJ, Lyle LT, Yeo Y. Nanosac, a noncationic and soft polyphenol nanocapsule, enables systemic delivery of siRNA to solid tumors. Acs Nano. 2021;15(3):4576-93.

26. Andhariya JV, Jog R, Shen J, Choi S, Wang Y, Zou Y, Burgess DJ. In vitro-in vivo correlation of parenteral PLGA microspheres: Effect of variable burst release. Journal of Controlled Release. 2019;314:25-37.

27. Habra K, Morris RH, McArdle SE, Cave GW. Controlled release of carnosine from poly (lactic-co-glycolic acid) beads using nanomechanical magnetic trigger towards the treatment of glioblastoma. Nanoscale Advances. 2022;4(10):2242-9.

28. Yamada S, Chai Y, Tagaya M. PEG functionalization effect of silicate-containing hydroxyapatite particles on effective collagen fibrillation with hydration layer state change. Physical Chemistry Chemical Physics. 2022;24(11):6788-802.

29. Mosmann T. Rapid colorimetric assay for cellular growth and survival: application to proliferation and cytotoxicity assays. Journal of immunological methods. 1983;65(1-2):55-63.

30. Kanamala M, Palmer BD, Jamieson SM, Wilson WR, Wu Z. Dual pH-sensitive liposomes with low pH-triggered sheddable PEG for enhanced tumor-targeted drug delivery. Nanomedicine. 2019;14(15):1971-89.